Electronic Structure of $ScC_6H_6^-$ and ScC_6H_6: Geometries, Electron Binding Energies, and Dyson Orbitals†

Srikanth Kambalapalli and J. V. Ortiz*

Department of Chemistry, Kansas State University, Manhattan, Kansas 66506-3701

Received: October 30, 2003; In Final Form: January 12, 2004

Ab initio, many-body methods are used to determine structures, relative energies, and vertical electron-detachment energies of $ScC_6H_6^-$. The two lowest anionic structures are singlets that display boat and inverse-boat conformations of the C_6H_6 ligand and have energies that are within 0.1 eV of each other. The principal peaks in a recently reported anion photoelectron spectrum are assigned to Dyson orbitals that are dominated by Sc 4s or $3d_{x^2-y^2}$ contributions in the boat form or by Sc 4s or $3d_{xy}$ contributions in the inverse-boat form. A triplet with C_{6v} symmetry is the third most stable state of the anion.

Introduction

Transition-metal complexes with benzene exemplify bonding relationships between d electrons and delocalized π orbitals.[1] Half-sandwich complexes with the formula MC_6H_6 are difficult to synthesize in a crystalline form, for their reactivity is enhanced by open metal coordination sites and partial occupation of frontier orbitals. Far more common are $M(C_6H_6)_2$ sandwich complexes and $ML_nC_6H_6$ complexes with monovalent L ligands that occupy coordination sites about the metal atom.

To characterize the electronic structure of the ground and excited states of MC_6H_6 complexes, several anion photoelectron spectra have been recorded.[2,3] These anions are inherently interesting also, for they may be considered complexes of transition-metal atoms in negative oxidation states with benzene molecules. $MC_6H_6^-$ species are prepared by reactions of laser-vaporized metal atoms with aromatic molecules in which metal plasmas, cooled by pulsed He gas, are allowed to react with He gas seeded with benzene. The resulting complex anions are accelerated by applying a pulsed electric field and are separated according to mass with a time-of-flight mass spectrometer. Photoelectron spectra are taken of the resulting, mass-selected anions. A report on the spectrum of the $ScC_6H_6^-$ anion provided a qualitative interpretation of the most prominent peaks, but no definite assignments were presented.[2]

Previously published quantum mechanical investigations on MC_6H_6 complexes have considered cationic species chiefly.[4−6] Recent density-functional calculations on neutral, cationic, and anionic complexes concentrated on ground-state properties, especially spin multiplicity of half-sandwich structures with C_{6v} symmetry.[7,8] Qualitative molecular orbital discussions of bonding between ML_n fragments and aromatic compounds have been based on extended Hückel calculations.[1,9,10]

In this report, ab initio calculations on $ScC_6H_6^-$ and ScC_6H_6 are performed to provide structural and energetic data on stable isomers of these species, to interpret the anion photoelectron spectrum and to obtain an orbital-based interpretation that relates the predicted properties to each other. Many-body methods, which are capable of describing the multiple kinds of bonding interactions that depend on electron correlation, are employed. Electron propagator theory[11] is an especially useful many-body formalism, for it efficiently provides Dyson orbitals that rigorously correspond to calculated electron-binding energies. Qualitative insights into chemical bonding and spectra may be obtained straightforwardly from the amplitudes and phase relationships of the Dyson orbitals.

Theoretical and Computational Methods

Geometry optimizations were performed at the MP2 level[12] and were followed by single-point coupled-cluster with single, double, and perturbative triple excitations (CCSD(T)) calculations.[13] The 6-311G** basis set for C and H atoms[14] and the 6-311+G* basis for the Sc atom were used.[15−17] Vertical electron detachment energies (VEDEs) were evaluated at optimized anion geometries with the ΔCCSD(T) approximation and with the outer-valence Green's function approximation (OVGF)[18−21] of electron propagator theory. In the latter calculations, the 6-311++G** basis[14−17,22] was used. All calculations were executed with Gaussian 98.[23]

For each anion VEDE that is calculated with electron propagator methods, there corresponds a Dyson orbital, $\Phi^{\text{Dyson}}(x)$, that is defined in terms of the initial N-electron and final $N-1$-electron states according to

$$\Phi^{\text{Dyson}}(x_1) = (N)^{1/2}\int \Psi_{\text{anion}}(x_1,x_2,x_3,x_4,\ldots,x_N)\,\Psi_{\text{neutral}}^{*}(x_2,x_3,x_4,\ldots,x_N)\,dx_2\,dx_3\,dx_4\ldots dx_N$$

where x_i is the combined spin−orbital coordinate of electron i. Each Dyson orbital describes how the electronic structure of an anionic, initial state differs from that of a neutral, final state. The pole strength, p, of a given VEDE is defined by

$$p = \int |\Phi^{\text{Dyson}}(x)|^2\,dx$$

and provides an index of the importance of electron correlation and orbital relaxation in determining the VEDE. Values of p between 1.0 and 0.8 indicate that the perturbative corrections to Koopmans's theorem, which are employed in the OVGF approximation, are qualitatively reasonable and are likely to produce useful assignments of spectra.

† Part of the special issue "Fritz Schaefer Festschrift".

* Author to whom correspondence may be addressed. E-mail: ortiz@ksu.edu.

10.1021/jp0312060 CCC: $27.50
Published on Web 02/13/2004

TABLE 1: MP2/6-311+G-Optimized Bond Lengths**

state	symmetry	configuration	C_1-C_2	C_2-C_3	C_1-H_1	C_2-H_2	$Sc-C_1$	$Sc-C_2$	Sc−Bz
$^1A_1$	C_{2v}	$(3d_{x^2-y^2})^2(4s)^2$	1.462	1.381	1.083	1.087	2.274	2.510	
$^1A_1$	C_{2v}	$(3d_{xy})^2(4s)^2$	1.407	1.489	1.089	1.084	2.518	2.352	
$^1A_1$	C_{6v}	$(3d_{xy})^2(3d_{x^2-y^2})^2$	1.457	1.457	1.088	1.088	2.255	2.255	1.721
$^3A_1$	C_{6v}	$(3d_{xy})^1(3d_{x^2-y^2})^1(4s)^2$	1.428	1.428	1.084	1.084	2.404	2.404	1.924
$^3A_2$	C_{2v}	$(3d_{x^2-y^2})^2(4s)^1(3d_{xy}{}^1)$	1.464	1.413	1.085	1.089	2.200	2.349	
$^3A_1$	C_{2v}	$(3d_{xy})^2(4s)^1(3d_{x^2-y^2})^1$	1.409	1.511	1.092	1.085	2.363	2.256	
$^2A_1$	C_{2v}	$(3d_{x^2-y^2})^2(4s)^1$	1.459	1.385	1.083	1.087	2.267	2.464	
$^2A_1$	C_{2v}	$(3d_{xy})^2(4s)^1$	1.406	1.489	1.088	1.084	2.473	2.323	
$^2A_2$	C_{2v}	$(3d_{xy})^1(4s)^2$	1.403	1.447	1.087	1.084	2.612	2.450	
$^2A_1$	C_{2v}	$(3d_{x^2-y^2})^1(4s)^2$	1.452	1.380	1.084	1.087	2.353	2.599	
$^4A_1$	C_{6v}	$(3d_{xy})^1(3d_{x^2-y^2})^1(4s)^1$	1.437	1.437	1.087	1.087	2.371	2.371	1.886

TABLE 2: MP2/6-311+G-Optimized Bond Angles and Dihedral Angles (deg)**

state	symmetry	configuration	$C_1-C_2-C_3$	$C_2-C_3-C_4$	H_1-C_1-Sc	$C_2-C_3-C_4-C_5$	$C_1-C_2-C_3-C_5$
$^1A_1$	C_{2v}	$(3d_{x^2-y^2})^2(4s)^2$	120.3	113.7	133.2	26.6	10.5
$^1A_1$	C_{2v}	$(3d_{xy})^2(4s)^2$	117.8	120.8	128.6	21.6	14.1
$^1A_1$	C_{6v}	$(3d_{xy})^2(3d_{x^2-y^2})^2$	120.0	120.0	131.1	0	0
$^3A_1$	C_{6v}	$(3d_{xy})^1(3d_{x^2-y^2})^1(4s)^2$	120.0	120.0	125.1	0	0
$^3A_2$	C_{2v}	$(3d_{x^2-y^2})^2(4s)^1(3d_{xy}{}^1)$	120.8	115.5	139.7	18.9	9.9
$^3A_1$	C_{2v}	$(3d_{xy})^2(4s)^1(3d_{x^2-y^2})^1$	117.8	122.6	129.6	15.9	7.6
$^2A_1$	C_{2v}	$(3d_{x^2-y^2})^2(4s)^1$	120.6	114.5	133.8	23	9.4
$^2A_1$	C_{2v}	$(3d_{xy})^2(4s)^1$	118.2	120.7	131.2	19.2	12.2
$^2A_2$	C_{2v}	$(3d_{xy})^1(4s)^2$	118.9	120.8	133.8	13.8	6.7
$^2A_1$	C_{2v}	$(3d_{x^2-y^2})^1(4s)^2$	114.3	119.9	130.1	26.8	14.2
$^4A_1$	C_{6v}	$(3d_{xy})^1(3d_{x^2-y^2})^1(4s)^1$	120.0	120.0	131.9	0	0

TABLE 3: $ScC_6H_6^-$ Total Energies and Vertical Electron-Detachment Energies

state	symmetry	UHF $\langle S^2\rangle$	total energy[a] +991. au	relative energy (eV)	orbital	VEDE[b] ΔCCSD(T) (eV)	VEDE[b] OVGF (eV)	OVGF pole strength	KT[c] (eV)
$^1A_1$	C_{2v}		−0.455533	0.000	4s	0.621	0.384	0.859	0.345
					$3d_{x^2-y^2}$	1.672	1.799	0.815	2.640
$^1A_1$	C_{2v}		−0.451271	0.116	4s	0.638	0.377	0.852	0.323
					$3d_{xy}$	1.293	1.532	0.806	2.450
$^1A_1$	C_{6v}		−0.372459	2.260	$3d_{xy}$	−0.6	−0.755	0.892	−0.732
					$3d_{x^2-y^2}$	−0.6	−0.754	0.892	−0.736
$^3A_1$	C_{6v}	2.16	−0.441109	0.392	α4s	0.631	0.388	0.912	0.077
					$\alpha 3d_{xy}$	1.489	1.308	0.795	2.355
					$\alpha 3d_{x^2-y^2}$	1.335	1.308	0.795	2.355
					β4s	0.512	0.281	0.818	0.705
$^3A_2$	C_{2v}	2.05	−0.436812	0.509	$\alpha 3d_{xy}$	0.352	0.402	0.866	0.645
					α4s	0.771	0.775	0.933	1.064
					$\alpha 3d_{x^2-y^2}$	0.970	1.204	0.882	1.418
					$\beta 3d_{x^2-y^2}$	1.07	1.053	0.868	1.305
$^3A_1$	C_{2v}	2.09	−0.432065	0.639	$\alpha 3d_{x^2-y^2}$	0.306	0.353	0.892	0.724
					α4s	0.268	0.859	0.922	1.177
					$\alpha 3d_{xy}$	1.123	1.083	0.855	1.235
					$\beta 3d_{xy}$	0.996	0.784	0.865	1.310

[a] Total energy from CCSD(T) calculations using 6-311++G** basis and geometry optimized at the MP2 level with 6-311G** basis on C_6H_6 and 6-311+G* basis on Sc. [b] Vertical electron-detachment energies of anions from calculations using 6-311++G** basis and geometry optimized at the MP2 level with 6-311G** basis on C_6H_6 and 6-311+G* basis on Sc. [c] Koopmans's theorem results.

Anion Structures and Energies

Geometry optimizations on the $ScC_6H_6^-$ anion are performed at the MP2 level with various reference electron configurations based on the C_{2v} and C_{6v} point groups. In each configuration, four electrons are assigned to metal-centered spin−orbitals generated by the Hartree−Fock self-consistent field. Molecular orbitals dominated by Sc 4s, $3d_{xy}$, or $3d_{x^2-y^2}$ functions are obtained in each case. In the C_{2v} point group, these orbitals are labeled a_1, a_2, and a_1, respectively; in the C_{6v} point group, the labels are a_1 for the Sc 4s-like molecular orbital and e_2 for the other two cases. Optimized bond lengths and angles corresponding to various reference configurations are displayed in Tables 1 and 2. Single-point CCSD(T) total energies and relative energies are shown in Table 3. Spin contamination in the triplet states, where unrestricted Hartree−Fock reference states are employed, is relatively low, and its effects are likely to be produced chiefly by quintet contributions, which are annihilated in the CCSD procedure. Additional data from MP2 optimizations is given in Table 4.

In optimizations restricted to C_{6v} symmetry (see Figure 1a), all Sc−C bond lengths and Sc−C−H bond angles are equivalent; the distances between the Sc atom and the distorted benzene ring's centroid (Sc−Bz) also are listed in Table 1. A slight bending of the benzene ring's H atoms toward the Sc atom takes place such that the planarity of the ligand is not completely conserved. The triplet with the $4s^2 3d_{xy} 3d_{x^2-y^2}$ ($a_1^2 e_2^2$) reference configuration is lower than the singlet with four 3d electrons. (Recent density-functional calculations concur on the relative stability of the triplet when C_{6v} symmetry is imposed and obtain a longer Sc−Bz distance of 2.08 Å.)[7,8] The out-of-plane bending of H atoms is approximately 2° in the triplet and 1° in the singlet.

TABLE 4: MP2/6-311+G-Optimized Total Energies of ScC_6H_6 and $ScC_6H_6^-$**

state	symmetry	configuration	UHF $\langle S^2 \rangle$	total energy (au)
$^2A_1$	C_{2v}	$(3d_{xy})^2(4s)^1$	0.7555	−991.340595
$^2A_1$	C_{2v}	$(3d_{x^2-y^2})^2(4s)^1$	0.7703	−991.344846
$^2A_2$	C_{2v}	$(3d_{xy})^1(4s)^2$	0.9258	−991.310244
$^2A_1$	C_{2v}	$(3d_{x^2-y^2})^1(4s)^2$	0.8076	−991.328492
$^2A_2$	C_{2v}	$(3d_{x^2-y^2})^2(3d_{xy})^1$	0.7883	−991.321864
$^2A_1$	C_{2v}	$(3d_{xy})^2(3d_{x^2-y^2})^1$	0.8039	−991.313000
$^4A_2$	C_{6v}	$(3d_{xy})^1(3d_{x^2-y^2})^1(4s)^1$	3.7571	−991.336897
$^1A_1$	C_{2v}	$(3d_{x^2-y^2})^2(4s)^2$		−991.358493
$^1A_1$	C_{2v}	$(3d_{xy})^2(4s)^2$		−991.355109
$^1A_1$	C_{6v}	$(3d_{xy})^2(3d_{x^2-y^2})^2$		−991.289480
$^3A_1$	C_{6v}	$(3d_{xy})^1(3d_{x^2-y^2})^1(4s)^2$	2.1609	−991.347195
$^3A_2$	C_{2v}	$(3d_{x^2-y^2})^2(4s)^1(3d_{xy})^1$	2.0514	−991.347533
$^3A_1$	C_{2v}	$(3d_{xy})^2(4s)^1(3d_{x^2-y^2})^1$	2.0907	−991.339631

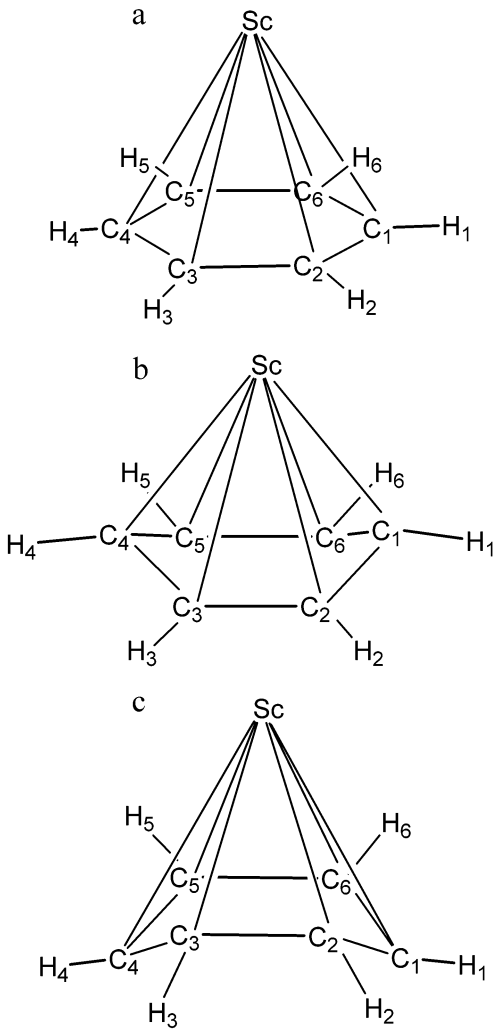

Figure 1. Structure of $ScC_6H_6^-$ complex with (a) C_{6v} symmetry, (b) C_{2v} symmetry and C_6H_6 boat structure, and (c) C_{2v} symmetry and C_6H_6 inverse-boat structure.

When the point group is reduced to C_{2v} in the optimizations, the benzene ligand distorts to boat (see Figure 1b) or inverse-boat (see Figure 1c) conformations. In the former case, two C atoms on opposite vertexes of the benzene ring have shorter distances to the Sc atom than the other four C atoms, whereas the latter case displays longer Sc−C distances for the same two C atoms. The two most stable structures have $4s^23d_{xy}^2$ and $4s^23d_{x^2-y^2}^2$ reference configurations and correspond to inverse-boat and boat geometries, respectively. These two singlets have approximately the same energy and are more stable than the two triplets with $4s3d^3$ configurations.

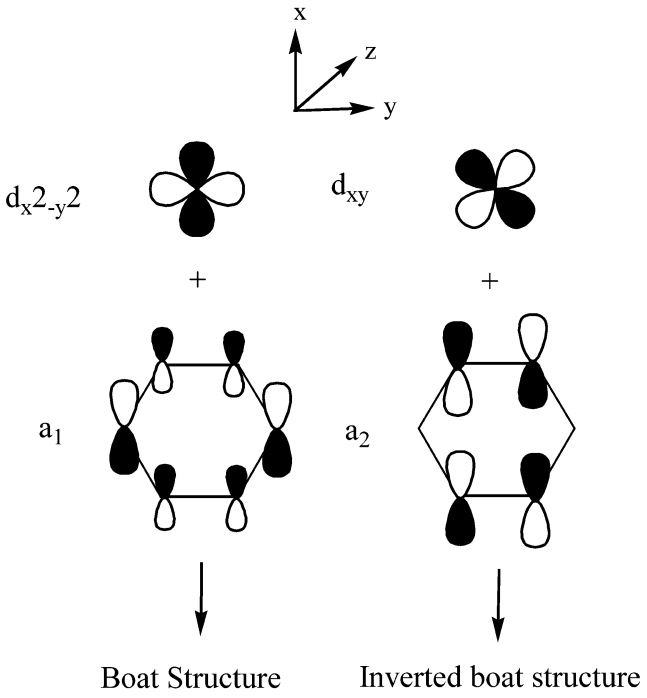

Figure 2. Schematic diagram for interaction of the $3d_{xy}$ and $3d_{x^2-y^2}$ orbitals of Sc with the a_1 and a_2 π^* antibonding orbitals of benzene in ScC_6H_6 and $ScC_6H_6^-$.

The accuracy of the total energy calculations does not permit a definitive determination of which C_{2v} singlet is the global minimum. However, these two states clearly are lower than the $4s^23d^2$ triplet with C_{6v} symmetry, the two $4s3d^3$ triplets with C_{2v} symmetry and the $3d^4$ singlet with C_{6v} symmetry. For the two $4s^23d^2$ singlets, the state with the higher number of $3d_{x^2-y^2}$ electrons is more stable by approximately 0.1 eV. Approximately the same amount of energy separates the two $4s3d^3$ triplets; the state with the larger number of $3d_{x^2-y^2}$ electrons also is favored.

In the singlet boat structure, four symmetry-equivalent Sc−C distances (see the first entry in the Sc−C_2 column of Table 1) are longer than the remaining two (Sc−C_1) Sc−C distances. The opposite trend is obtained in the inverse-boat singlet (see the second entries in the same columns). Stabilizing delocalization with in-phase relationships between the 3d orbitals and the π^* orbitals of benzene produces stronger Sc−C bonding and shorter Sc−C distances. Figure 2 displays the phase relationships in the two molecular orbitals dominated by $3d_{x^2-y^2}$ and $3d_{xy}$ contributions.

When two electrons are assigned to the a_1 molecular orbital dominated by Sc $3d_{x^2-y^2}$, delocalization into the a_1 π^* orbital of benzene contributes to C_1-C_2 antibonding and C_2-C_3 bonding relationships. Assignment of two electrons to the a_2 molecular orbital with large Sc $3d_{xy}$ character and some delocalization into the a_2 π^* orbital of benzene accentuates C_2-C_3 antibonding relationships. Therefore, optimization with the $4s^23d_{x^2-y^2}^2$ configuration produces a boat structure with shorter C_2-C_3 distances and longer C_1-C_2 distances than optimization with the $4s^23d_{xy}^2$ configuration, which produces an inverse-boat structure.

Comparisons with the bond lengths of the remaining anion structures usually confirm the qualitative trends suggested by the phase relationships that are obtained in the $3d_{xy}$ (a_2) and $3d_{x^2-y^2}$ (a_1) molecular orbitals. Shorter Sc−C bond lengths occur in the $3d^4$ singlet and in the two $4s3d^3$ triplets than in the two $4s^23d^2$ singlets. Starting from the $4s^23d_{x^2-y^2}^2$ singlet state, the transfer of a 4s electron to the $3d_{xy}$ orbital produces a triplet

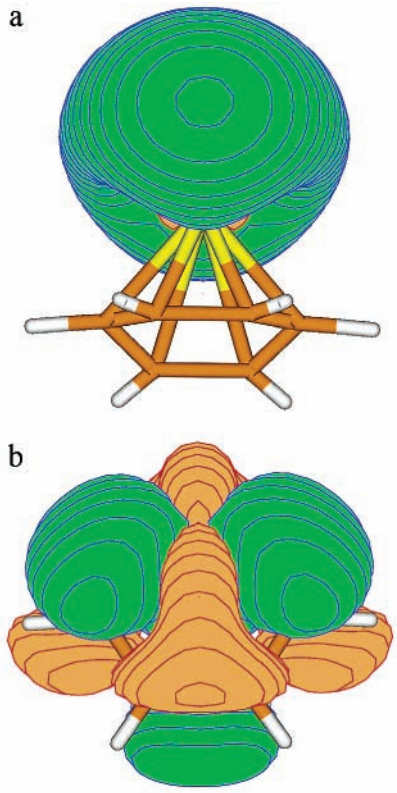

Figure 3. Dyson orbitals for VEDEs of the C_{2v} boat form of $ScC_6H_6^-$. (a) $^1A_1$ $4s^23d_{x^2-y^2}{}^2$ $ScC_6H_6^- \rightarrow {}^2A_1$ $4s3d_{x^2-y^2}{}^2$ ScC_6H_6. (b) $^1A_1$ $4s^23d_{x^2-y^2}{}^2$ $ScC_6H_6^- \rightarrow {}^2A_1$ $4s^23d_{x^2-y^2}$ ScC_6H_6.

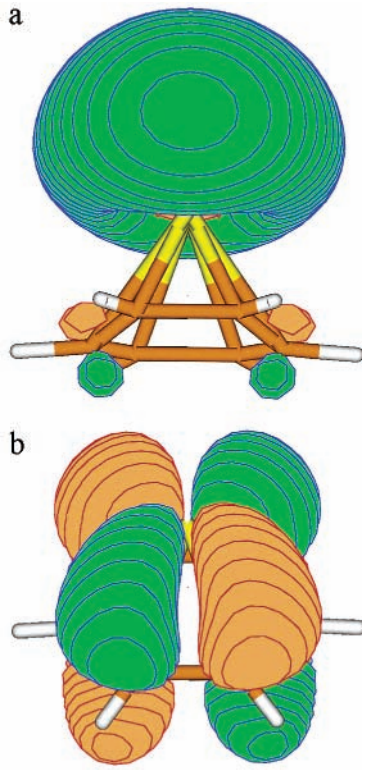

Figure 4. Dyson orbitals for VEDEs of the C_{2v} inverse-boat form of $ScC_6H_6^-$. (a) $^1A_1$ $4s^23d_{xy}{}^2$ $ScC_6H_6^- \rightarrow {}^2A_1$ $4s3d_{xy}{}^2$ ScC_6H_6. (b) $^1A_1$ $4s^2$-$3d_{xy}{}^2$ $ScC_6H_6^- \rightarrow {}^2A_2$ $4s^23d_{xy}$ ScC_6H_6.

with longer C_2-C_3 bond lengths. However, a similar transfer involving the $4s^23d_{xy}{}^2$ singlet and the $4s3d_{xy}{}^23d_{x^2-y^2}$ triplet also produces longer C_2-C_3 bond lengths in the triplet, despite the C_2-C_3 bonding phase relationship that the $3d_{x^2-y^2}$ orbital exhibits, and has no significant effect on the C_1-C_2 bond lengths, despite the antibonding phase relationships displayed by the same orbital. Comparison of the singlet $3d^4$ C_{6v} singlet and the $3d^24s^2$ C_{6v} triplet shows smaller Sc−C distances in the former case. This trend is compatible with the bonding Sc−C interactions of the $3d_{xy}$ (a_2) and $3d_{x^2-y^2}$ (a_1) orbitals. The nonbonding character of the molecular orbital dominated by Sc 4s contributions increases the Sc atomic radius and also contributes to the trends in Sc−C distances.

Vertical Electron Detachment Energies

To assign anion photoelectron spectra, VEDEs of the anions are calculated with OVGF and ΔCCSD(T) calculations. The former method provides a direct determination of the VEDE, a Dyson orbital corresponding to the transition, and a pole strength. VEDEs are listed for each anion in Table 3. Dyson orbitals corresponding to the VEDEs of the two lowest singlets are shown in Figures 3 (boat form of C_6H_6) and 4 (inverse-boat form of C_6H_6). For both structures, the first VEDE corresponds to a Dyson orbital that consists chiefly of Sc 4s contributions and that exhibits little delocalization onto the C_6H_6 ligand. The remaining Dyson orbitals in Figures 3 and 4 display bonding relationships between Sc 3d and benzene π^* orbitals. OVGF pole strengths above 0.8 confirm the qualitative validity of perturbative improvements to Koopmans's theorem results and the proportionality of the Dyson orbitals to canonical Hartree−Fock orbitals.

Calculated VEDEs for the most stable (boat) structure, which has the singlet, $4s^23d_{x^2-y^2}{}^2$ configuration, are in close agreement with the first and third peaks in the experimental photoelectron spectrum, which occur at 0.64 and 1.82 eV, respectively.[2] Relaxation and correlation corrections to the results of Koopmans's theorem are especially large for the higher VEDE. Because the total energy of the second most stable (inverse-boat) structure, with the singlet, $4s^23d_{xy}{}^2$ configuration, is so close to that of the lowest structure, the ion-source conditions of the experimental apparatus are capable of producing a spectrum that represents a mixture of the two structures. Values for the VEDEs of the second most stable structure in Table 3 are in close agreement with the first and second peaks in the observed spectrum, which occur at 0.64 and 1.37 eV, respectively.[2] Corrections to Koopmans's theorem results also are large for the higher VEDE of the second structure. There is little difference between the lowest VEDEs of the two structures. This result is compatible with the larger intensity of the first peak, which is approximately two times as large as the intensities of the second and third peaks.

Whereas the latter peaks exhibit many subpeaks and shoulders, the first peak is relatively sharp. The onset of electron detachment occurs at 0.49 eV in the observed spectrum,[2] indicating a final-state relaxation energy associated with nuclear displacements of approximately 0.15 eV. These features also are compatible with the qualitative descriptions of the Dyson orbitals. Removal of an electron from the a_1 molecular orbital dominated by Sc 4s contributions has little effect on the structure of the C_6H_6 ligand, but a reduction of ligand−metal distances, produced by the smaller size of the Sc atom, does occur. In contrast, removal of an electron from the $3d_{xy}$ or $3d_{x^2-y^2}$ orbitals causes increased metal−ligand distances and changes in C−C bond lengths. In the former case, removal of a $3d_{xy}$ electron reduces C_2-C_3 antibonding relationships and produces shorter C_2-C_3 distances. When an electron is removed from a $3d_{x^2-y^2}$ orbital, C_1-C_2 antibonding relationships are diminished and a reduction of the C_1-C_2 bond lengths takes place.

Calculations on the VEDEs of some of the less stable anionic species are not in agreement with the experimental data. For the C_{6v} singlet, the VEDEs have the wrong sign. The $4s3d^3$ triplets are predicted to have VEDEs corresponding to final-state quartets in energy regions where there are no peaks. Other VEDEs are predicted at values that are too low with respect to the first observed peak at 0.64 eV. The C_{6v} triplet VEDEs are in reasonable agreement with the first and second observed peaks, but the relative energy of the triplet, 0.39 eV above the lowest singlet, makes it unlikely to be present in the experimental sample.

ScC_6H_6 Structures

Qualitative predictions on structural changes accompanying electron detachment from anionic states that are based on the phase relationships in the Dyson orbitals are confirmed by geometry optimizations on uncharged complexes. Comparison of Sc−C and C−C bond lengths in uncharged states with $4s3d^2$ and $4s^23d$ configurations (see Table 1) with corresponding information for the two most stable singlets of the anion shows that Sc−C distances depend strongly on the number of electrons in 4s-dominated a_1 molecular orbitals and that the structure of the C_6H_6 ligand is almost unaffected by the occupation number of the same molecular orbital. However, changes in the number of electrons in $3d_{xy}$ or $3d_{x^2-y^2}$ orbitals affect metal−ligand and C−C bond lengths.

Optimized MP2 energies for doublet and quartet states with various reference configurations are shown in Table 4. The most stable structures are C_{2v} doublets with $4s3d^2$ configurations; the $4s3d_{x^2-y^2}{}^2$ total energy is approximately 0.1 eV lower than the $4s3d_{xy}{}^2$ total energy. A C_{6v}, quartet state with three α electrons in the 4s, $3d_{x^2-y^2}$, and $3d_{xy}$ orbitals is the third most stable structure. (Density-functional calculations on the C_{6v} quartet[7,8] obtain a Sc−Bz distance of 2.00 Å that is considerably longer than the present value of 1.89 Å.) In these three states, expectation values of S^2 are close to their exact values, 0.75 for doublets and 1.75 for quartets, in the unrestricted Hartree−Fock reference determinant. However, such calculations on doublets with three electrons assigned to the same three orbitals produce unacceptably large spin contamination, and the corresponding relative energies cannot be considered reliable. The remaining doublets with $4s^23d$ or $3d^3$ configurations lie at higher energies.

Conclusions

Two C_{2v} singlet anions with boat and inverted-boat structures for the C_6H_6 ligand are separated by approximately 0.1 eV, with the boat structure being lower. The distortion of the benzene ring to the boat and inverted-boat structures is produced by doubly occupied $3d_{x^2-y^2}$ and $3d_{xy}$ orbitals, respectively, with Sc−C bonding delocalization into π^* benzene orbitals. In these two states, the least-bound electrons are assigned to closed-shell $4s^23d^2$ configurations. The molecular orbitals dominated by Sc 4s contributions exhibit little delocalization into the C_6H_6 ligand and changes in their occupation numbers accompanying ionization or excitation do not produce major changes in C−C bond lengths. However, such changes do affect the size of the Sc atom, and therefore, Sc−C distances increase with the number of electrons assigned to the Sc 4s-like molecular orbital.

VEDEs corresponding to the 4s and $3d_{x^2-y^2}$ orbitals of the boat form and to the 4s and $3d_{xy}$ orbitals of the inverted-boat form suffice to explain the three principal peaks of the photoelectron spectrum of $ScC_6H_6^-$. The 4s VEDEs of the two isomers are almost equal and account for the larger intensity associated with the lowest peak in the photoelectron spectrum. The second VEDE of the anion with the boat ligand is larger than the second VEDE of the anion with the inverted-boat ligand. The former structure has the lower total energy and corresponds to the first and third principal peaks of the anion photoelectron spectrum. The inverted-boat structure is slightly less stable and corresponds to the first and second peaks. The sharpness of the first peak is a consequence of the absence of C−C bonding relationships in the Dyson orbitals accompanying the first VEDE of both anions.

In contrast, the vibronically structured second and third peaks are consequences of C−C bonding and antibonding relationships found in the second VEDE of the boat and inverse-boat isomers of $ScC_6H_6^-$. Changes in Sc−C and C−C distances accompanying electron detachment from the anionic states are related to the amplitudes, especially interatomic phase relationships, in the corresponding Dyson orbitals.

Acknowledgment. The National Science Foundation (Grant CHE-0135823) and the Petroleum Research Fund of the American Chemical Society (Grant 34859-AC6) provided support for this research.

References and Notes

(1) Muetterties, E. L.; Bleeke, J. R.; Wucherer, E. J.; Albright, T. A. *Chem. Rev.* **1982**, *82*, 499 and references therein.

(2) Judai, K.; Nakamura, Y.; Tachibana, M.; Negishi, Y.; Nakajima, A.; Kaya, K. *Chem. Lett.* **2001**, 114.

(3) Kurikawa, T.; Takeda, H.; Hirano, M.; Judai, K.; Arita, T.; Nagao, S.; Nakajima, A.; Kaya, K. *Organometallics* **1999**, *18*, 1430.

(4) Bauschlicher, C. W.; Partridge, H.; Langhoff, S. R. *J. Phys. Chem.* **1992**, *96*, 3273.

(5) Chaquin, P.; Costa, D.; Lepetit, C.; Che, M. J. *Phys. Chem. A* **2001**, *105*, 4541.

(6) Yang, C.; Klippenstein, S. J. *J. Phys. Chem. A* **1999**, *103*, 1094.

(7) Pandey, R.; Rao, B. K.; Jena, P.; Newsam, J. M. *Chem. Phys. Lett.* **2000**, *321*, 142.

(8) Pandey, R.; Rao, B. K.; Jena, P.; Blanco, M. A. *J. Am. Chem. Soc.* **2001**, *123*, 3799.

(9) Wexler, P. A.; Wigley, D. E.; Koerner, J. B.; Albright, T. A. *Organometallics* **1991**, *10*, 2319.

(10) Elian, M.; Chen, Maynard M. L.; Mingos, D. M. P.; Hoffman, R. *Inorg. Chem.* **1976**, *15*, 1148.

(11) Ortiz, J. V. *Adv. Quantum Chem.* **1999**, *35*, 33 and references therein.

(12) Møller, C.; Plesset, M. S. *Phys. Rev.* **1934**, *46*, 618.

(13) Ragavachari, K.; Trucks, G. W.; Pople, J. A.; Head-Gordon, M. *Chem. Phys. Lett.* **1989**, *157*, 479.

(14) Hehre, W. J.; Ditchfield, R.; Pople, J. A. *J. Chem. Phys.* **1972**, *56*, 2257.

(15) Wachters, A. J. H. *J. Chem. Phys.* **1970**, *52*, 1033.

(16) Hay, P. J. *J. Chem. Phys.* **1977**, *66*, 4377.

(17) Raghavachari, K.; Trucks, G. W. *J. Chem. Phys.* **1989**, *91*, 1062.

(18) Cederbaum, L. S. *J. Phys. B* **1975**, *8*, 290.

(19) Von Niessen, W.; Schirmer, J.; Cederbaum, L. S. *Comput. Phys. Rep.* **1984**, *1*, 57.

(20) Zakrzewski, V. G.; Ortiz, J. V.; Nichols, J. A.; Heryadi, D.; Yeager, D. L. *Int. J. Quantum Chem.* **1996**, *60*, 29.

(21) Ortiz, J. V.; Zakrzewksi, V. G.; Dolgounitcheva, O. In *Conceptual Perspectives in Quantum Chemistry*; Calais, J.-L., Kryachko, E., Eds.; Kluwer: Dordrecht, 1997; Vol. 3, p 465.

(22) Clark, T.; Chandrasekhar, J.; Spitznagel, G. W.; Schleyer, P. v. R. *J. Comput. Chem.* **1983**, *4*, 294.

(23) Frisch, M. J.; Trucks, G. W.; Schlegel, H. B.; Scuseria, G. E.; Robb, M. A.; Cheeseman, J. R.; Zakrzewski, V. G.; Montgomery, J. A., Jr.; Stratmann, R. E.; Burant, J. C.; Dapprich, S.; Millam, J. M.; Daniels, A. D.; Kudin, K. N.; Strain, M. C.; Farkas, O.; Tomasi, J.; Barone, V.; Cossi, M.; Cammi, R.; Mennucci, B.; Pomelli, C.; Adamo, C.; Clifford, S.; Ochterski, J.; Petersson, G. A.; Ayala, P. Y.; Cui, Q.; Morokuma, K.; Malick, D. K.; Rabuck, A. D.; Raghavachari, K.; Foresman, J. B.; Cioslowski, J.; Ortiz, J. V.; Stefanov, B. B.; Liu, G.; Liashenko, A.; Piskorz, P.; Komaromi, I.; Gomperts, R.; Martin, R. L.; Fox, D. J.; Keith, T.; Al-Laham, M. A.; Peng, C. Y.; Nanayakkara, A.; Gonzalez, C.; Challacombe, M.; Gill, P. M. W.; Johnson, B. G.; Chen, W.; Wong, M. W.; Andres, J. L.; Head-Gordon, M.; Replogle, E. S.; Pople, J. A. *Gaussian 98*, revision A.7; Gaussian, Inc.: Pittsburgh, PA, 1998.